

# Towards Adaptive Visual Token Pruning for Large Multimodal Models

Hao Zhang<sup>1\*</sup>, Mengsi Lyu<sup>1\*</sup>, Chenrui He<sup>1</sup>, Yulong Ao<sup>1†</sup>, Yonghua Lin<sup>1†</sup>

<sup>1</sup>Beijing Academy of Artificial Intelligence

## Abstract

Large Multimodal Models (LMMs) have achieved significant success across various tasks. These models usually encode visual inputs into dense token sequences, which are then concatenated with textual tokens and jointly processed by a language model. However, the increased token count substantially raises computational and memory costs during inference. Token pruning has emerged as a promising approach to address this issue. Existing token pruning methods often rely on costly calibration or suboptimal importance metrics, leading to redundant retained tokens. In this paper, we analyze the redundancy differences between visual and textual tokens and propose pruning exclusively on visual tokens. Based on this, we propose a visual token pruning strategy that explicitly preserves both cross-modal alignment and intra-modal informational diversity. We introduce a mutual information-based token pruning strategy that removes visual tokens semantically misaligned with textual tokens, effectively preserving the alignment between the visual and textual modalities. To further improve the representational quality of the retained tokens, we additionally prune redundant visual tokens by maximizing the expected pairwise distances in the embedding space, which is solved efficiently with a greedy algorithm. Extensive experiments demonstrate that our method maintains strong performance while reducing tokens by 88.9% on models such as LLaVA-1.5-7B and LLaVA-NEXT-7B, resulting in a 56.7% improvement in inference speed.

## Introduction

Large Multimodal Models (LMMs) (Bai et al. 2025; Team et al. 2025; Zhu et al. 2025; Liu et al. 2024a; Lin et al. 2023) have substantially enhanced the reasoning capabilities of Large Language Models (LLMs) (Brown et al. 2020; Touvron et al. 2023; Chiang et al. 2023; Zhu et al. 2023; Li et al. 2023a; Zhang et al. 2023; Huang et al. 2023; Wang et al. 2023) by enabling joint processing of multimodal inputs such as images and texts. Typically, visual inputs are encoded into dense token sequences via a vision encoder and concatenated with textual tokens for unified processing by the language model. However, the resulting token sequences often reach thousands in length, leading to significant computational and memory overhead due to the quadratic complexity of self-attention with respect to sequence length (Vaswani et al.

2017; Face 2024; Chen et al. 2023; Keles, Wijewardena, and Hegde 2023; Liu et al. 2022). These limitations present major obstacles to deploying LMMs in resource-constrained or latency-sensitive environments (Chen et al. 2024a; Lin et al. 2025a).

Recent studies have shown that visual token representations in LMMs exhibit substantial redundancy (Liu et al. 2024c; Shang et al. 2024a; Huang et al. 2024; Tong et al. 2025; Li, Yang, and Lu 2025). Leveraging this insight, visual token pruning methods have been proposed to reduce computational cost by selectively removing unnecessary tokens. By eliminating redundant visual tokens, these approaches effectively alleviate the quadratic burden of long input sequences. Notably, prior work demonstrates that pruning the majority of visual tokens can yield significant efficiency gains with minimal performance degradation (Zhang et al. 2024a; Chen et al. 2024a; Lin et al. 2025a; Huang et al. 2024; Sun et al.).

While token pruning is beneficial, its application to LMMs remains challenging. Existing token pruning methods can be broadly categorized into three types. 1) A common approach is to use attention scores to identify redundant tokens (Chen et al. 2024b; Lin et al. 2025b; Shang et al. 2024b; Tong et al. 2025). However, such methods are susceptible to positional bias and often retain spatially adjacent tokens with high similarity, leading to redundancy and performance degradation. 2) Other methods rely on model-specific calibration or fine-tuning (Ye et al. 2025; Lin et al. 2025b; Li et al. 2025b; Cai et al. 2024), which incurs high computational cost and limits scalability in practical deployment. 3) Another line of work addresses token pruning by maximizing the minimum distance between tokens (Alvar et al. 2025). While this strategy encourages token separation, it is sensitive to outliers and may fail to preserve cross-modal alignment, ultimately affecting downstream performance.

In view of these challenges and opportunities, we propose a visual token pruning strategy that explicitly preserves both cross-modal alignment and intra-modal informational diversity. Our analysis begins by examining the inherent redundancy differences between visual and textual tokens through three key perspectives: attention mechanisms, semantic distribution, and information repetition. These analyses reveal that visual tokens exhibit significantly higher redundancy compared to their textual counterparts. Consequently, we choose to prune only visual tokens while retaining all textual

\*These authors contribute equally to this work.

†Corresponding author.

tokens. To preserve cross-modal alignment during pruning, we estimate the mutual information between visual and textual token embeddings. Visual tokens with higher expected mutual information with textual tokens are more likely to exhibit semantic alignment with the textual modality and are therefore retained, while those with lower mutual information are pruned as misaligned. Additionally, we retain visual tokens by maximizing their expected pairwise distances in the embedding space, thereby promoting intra-modal information diversity and encouraging rich, non-overlapping visual semantic representations. To address this problem efficiently, we employ a greedy algorithm that iteratively selects tokens exhibiting maximal dissimilarity. Extensive experiments demonstrate that our method maintains strong performance while reducing tokens by 88.9% on models such as LLaVA-1.5-7B and LLaVA-NEXT-7B, resulting in a 56.7% improvement in inference speed. In summary, our contributions can be summarized as follows:

- We analyze the redundancy differences between visual and textual tokens and propose pruning exclusively on visual tokens. Based on this, we design a visual token pruning method that explicitly preserves cross-modal alignment and intra-modal information diversity, improving inference efficiency while maintaining semantic integrity.
- We introduce a mutual information based pruning strategy that retains semantically aligned visual tokens with textual tokens while removing misaligned ones, effectively preserving the alignment between visual and textual modalities.
- We propose an information diversity driven pruning strategy that maximizes the expected pairwise distances among visual tokens in the embedding space, effectively reducing redundancy and enhancing intra modal information richness, which is solved efficiently with a greedy algorithm.

## Related Work

**Large Multimodal Models (LMMs)** extend pretrained LLMs by integrating multiple modalities (Bai et al. 2025; Team et al. 2025), such as images and texts. Typically, a vision encoder extracts dense visual features, which are projected into the language model’s embedding space via modules like Q-Former (Chebotar et al. 2023) or MLPs (Taud and Mas 2017). Conventional methods resize high-resolution images to a fixed scale (Koonce 2021), causing geometric distortions and loss of fine-grained spatial details. Dynamic tiling mitigates this by splitting images into smaller regions, each independently encoded by a shared encoder, better preserving local information (Yuan et al. 2021; Yin et al. 2022). However, this increases the number of visual tokens and computational cost, a challenge further amplified in video LMMs due to multi-frame processing (Liu et al. 2024c). These challenges highlight the need for efficient inference methods to enable LMMs deployment under resource constraints (Tong et al. 2025).

**Visual Token Pruning** aims to reduce computational overhead and improve inference efficiency by removing redundant or less informative visual tokens. A common strategy

is to leverage attention scores to identify tokens for removal. For example, PruMerge (Shang et al. 2024b) clusters and merges tokens in the vision encoder based on attention sparsity, while FastV (Chen et al. 2024a) utilizes attention weights from the second layer of the LLM to guide pruning. SparseVLM (Zhang et al. 2024b) employs cross-modal attention for text-conditioned token selection, and VisionZip (Yang et al. 2025) compresses visual inputs via CLS token attention in the final vision encoder layer. FlowCut (Tong et al. 2025) identifies redundancy from an information flow perspective by analyzing attention propagation. LVPPruning (Sun et al. 2025) uses cross-attention to assess vision token importance via interaction with language tokens, guiding token pruning. Other methods adopt calibration-based strategies, where pruning ratios and depths are determined by evaluating model behavior on a held-out set. FitPrune (Ye et al. 2025) compares attention distributions before and after pruning to inform token selection, while VTW (Lin et al. 2025a) shows that tokens can be safely dropped after specific layers, guided by calibration. In addition, approaches like DivPrune (Alvar et al. 2025) addresses token pruning by maximizing the minimum distance between tokens. Moreover, a concurrent work (Zhang et al. 2025) reformulates the token pruning problem using determinantal point processes to achieve effective pruning.

## Token Redundancy Across Modalities

Previous studies have yet to systematically and thoroughly compare token redundancy across different modalities (Shang et al. 2024a; Alvar et al. 2025; Li, Yang, and Lu 2025). In this section, we analyze and contrast the redundancy of textual and visual tokens from **three perspectives: attention mechanisms, semantic distribution and information repetition**. Our findings reveal that visual tokens exhibit substantially higher redundancy than textual tokens. Motivated by this observation, we retain all textual tokens during the token pruning process and apply pruning exclusively to visual tokens.

The attention distribution in multimodal models is highly skewed, with textual tokens receiving significantly higher weights than visual tokens (Li et al. 2025a; Lee et al. 2025). This suggests that the model primarily relies on text for semantic understanding. Visual inputs often consist of hundreds or thousands of tokens, far exceeding the number of textual tokens. Given the quadratic complexity of attention with respect to token count, this mismatch between quantity and contribution is pronounced. Despite the large number of visual tokens, their impact on the final representation is limited, resulting in poor trade offs between computational cost and semantic gain and reflecting the high redundancy of visual tokens.

Each token in text typically carries explicit semantic meaning, such as a noun, verb, or conjunction, reflecting natural language as a highly optimized discrete encoding system with dense and relatively uniform information distribution (Hirschberg and Manning 2015). In contrast, semantic information in images is highly concentrated in a small number of salient regions, such as foreground objects, while the majority of visual tokens correspond to low-semantic areas like

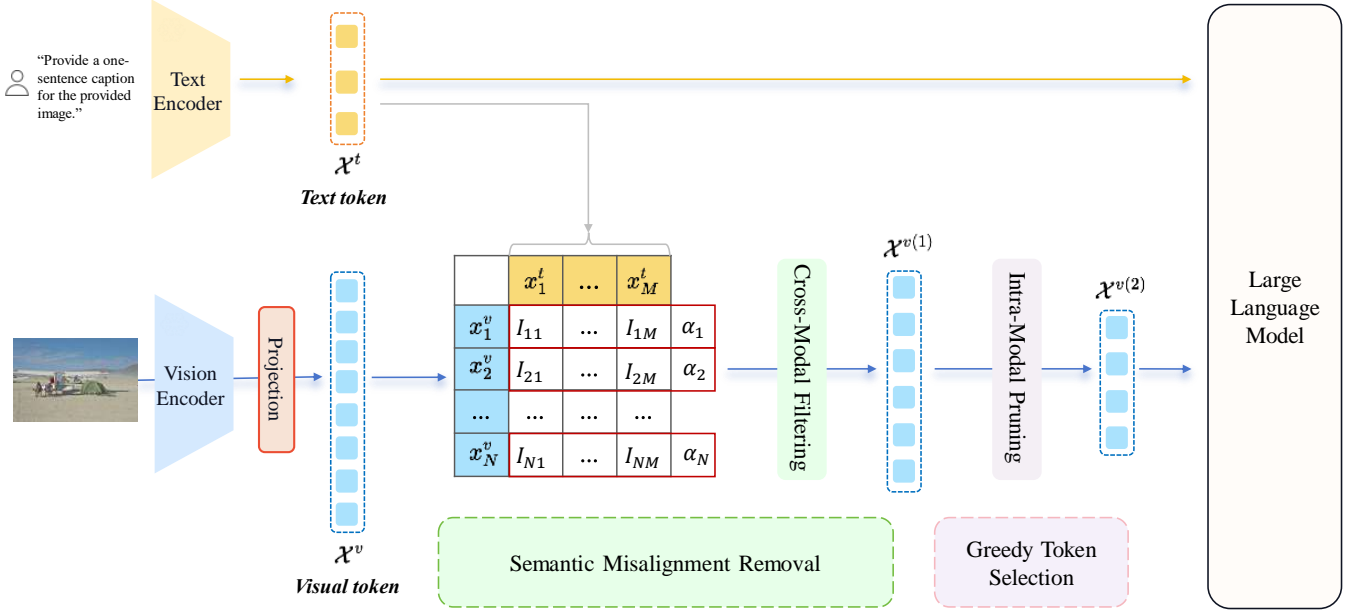


Figure 1: Overview of the visual token pruning method. Visual tokens that exhibit low semantic alignment with textual tokens are pruned by measuring their cross-modal mutual information. The remaining tokens are further reduced by maximizing the intra-modal representation within the visual modality, which is efficiently solved using a greedy algorithm.

sky or walls, which mostly contain low-frequency textures or superficial variations and contribute little to high-level semantic understanding. Consequently, the effective semantic density of visual tokens is significantly lower than that of textual tokens.

Compared to textual tokens, visual tokens exhibit higher information redundancy due to differences in their generation processes and underlying information structures. Textual tokens, derived from natural language, follow Zipf's law (Newman 2005; Adamic and Huberman 2002) and represent distinct semantic units with low repetition. In contrast, visual tokens are typically generated by uniformly partitioning images or extracting low-level features without semantic organization. For example, a sky region is divided into multiple similar patches that cluster in embedding space and jointly represent a single high-level concept, causing redundancy. Visual tokenization resembles physical partitioning rather than frequency-driven semantic abstraction, forcing models to process many similar tokens and resulting in computational and representational inefficiency.

## Methodology

### Problem Formulation

In this section, we propose a visual token pruning strategy that explicitly preserves cross-modal alignment while promoting intra-modal information diversity. Given an input image, we extract a sequence of visual tokens  $X^v = \{x_1^v, \dots, x_N^v\}$ , and embed the accompanying text into a sequence of textual tokens  $X^t = \{x_1^t, \dots, x_M^t\}$ , where  $x_i^v, x_j^t \in \mathbb{R}^d$ .

Our pruning pipeline can be roughly divided into two

stages. In the first stage, we select a subset  $X^{v(1)} \subset X^v$  with size  $|X^{v(1)}| = N_1$ , where  $N_1 < N$ , by retaining tokens with the highest semantic alignment to the text modality, thereby ensuring the preservation of tokens with strong cross-modal correlations. In the second stage, we further prune  $X^{v(1)}$  to obtain a more compact subset  $X^{v(2)} \subset X^{v(1)}$  with size  $|X^{v(2)}| = N_2$ , where  $N_2 < N_1$ , by maximizing the expected pairwise distance in the embedding space. This promotes non-redundant and information-rich representations while reducing computational overhead. Figure 1 illustrates the overall architecture of our method.

### Cross-Modal Alignment Aware Token Filtering

During training, multimodal models primarily optimize cross-entropy loss for text generation, which often leads to an implicit weakening of cross-modal alignment (Covert et al. 2024). Pruning as a post-processing step for the model is crucial for cross-modal alignment. To preserve cross-modal alignment during visual token pruning, we introduce a mutual information based criterion that selects a subset of visual tokens  $X^{v(1)}$  which maximizes the expected mutual information with the textual tokens. Our selection objective can be formulated as follows:

$$X^{v(1)} = \arg \max_{X^{v'} \subset X^v, |X^{v'}|=N_1} \mathbb{E}_{x^t \in X^t} [I(X^{v'}; x^t)] \quad (1)$$

Here,  $X^{v'}$  serves as a temporary variable.  $I(X^{v'}; x^t)$  denotes the average mutual information between the textual token  $x^t$  and all visual tokens in the subset  $X^{v'}$ . Furthermore, we define the alignment score  $\alpha_i$  of each visual token  $x_i^v$  based on its mutual information with the textual token set

$X^t$  as follows:

$$\alpha_i = I(x_i^v; X^t) = \frac{1}{M} \sum_{j=1}^M I(x_i^v; x_j^t) \quad (2)$$

This score can be interpreted as the inverse of the InfoNCE loss (Rusak et al. 2024), reflecting the average semantic alignment strength of visual tokens within the shared embedding space. Intuitively, tokens with higher alignment scores are retained, while those with lower semantic alignment are pruned.

Although mutual information provides a theoretically grounded measure of cross-modal alignment, its precise estimation in high dimensional spaces often requires costly density modeling. We approximate mutual information using the  $L_2$  norm, which reduces computational overhead without compromising performance. It is worth noting that our approximation is grounded in mathematical theory and does not rely on any specific model architecture. **Additionally, we provide theoretical justification and experimental analysis to explain why the  $L_2$  norm is used for approximation instead of other metrics (see Appendix 1 and 2).** Therefore, we can compute  $\alpha_i$  using the following formula:

$$\alpha_i = -\frac{1}{M} \sum_{j=1}^M \|x_i^v - x_j^t\|_2 \quad (3)$$

We then construct the set  $X^{v(1)}$  by selecting the  $N_1$  visual tokens with the highest alignment scores, which can be represented as follows:

$$X^{v(1)} = \{x_i^v \in X^v \mid \alpha_i \in \text{top}_{N_1}(\alpha_1, \alpha_2, \dots, \alpha_N)\} \quad (4)$$

This selection effectively filters out semantically misaligned visual tokens while retaining those with the strongest cross-modal correlations, thereby enhancing alignment quality and reducing computational overhead.

### Intra-Modal Representational Maximization

After obtaining the visual token set  $X^{v(1)}$ , we select a refined subset  $X^{v(2)}$  by explicitly maximizing intra-modal information diversity. The core idea is to retain a set of visual tokens that are semantically diverse and non-redundant. To achieve this, we maximize the expected pairwise distance among the selected tokens. Specifically, we define the distance between two visual tokens  $x_i^v$  and  $x_j^v$  using cosine dissimilarity. Based on this, we formulate the objective for subset selection as follows:

$$D(x_i^v, x_j^v) = 1 - \frac{(x_i^v)^\top x_j^v}{\|x_i^v\|_2 \cdot \|x_j^v\|_2} \quad (5)$$

$$X^{v(2)} = \arg \max_{\tilde{\mathcal{X}} \subset X^{v(1)}, |\tilde{\mathcal{X}}|=N_2} \mathbb{E}_{x_i^v, x_j^v \in \tilde{\mathcal{X}}, i \neq j} [D(x_i^v, x_j^v)] \quad (6)$$

This objective encourages the model to retain visual tokens that capture complementary aspects of the input, thereby enhancing the representational richness of the pruned token set. To address the problem, we introduce a binary selection vector  $\gamma \in \{0, 1\}^{N_1}$ . The objective can be expressed as

follows:

$$\max_{\gamma \in \{0, 1\}^{N_1}} \sum_{i=1}^{N_1} \sum_{j=1, j \neq i}^{N_1} \gamma_i \gamma_j \cdot D(x_i^v, x_j^v), \quad \sum_{i=1}^{N_1} \gamma_i = N_2 \quad (7)$$

The above problem is a combinatorial optimization task, which is known to be NP Hard. To address this, we adopt an efficient greedy algorithm for approximate optimization. The core idea is to iteratively select the next visual token that is farthest from the current selected subset in the embedding space, thereby progressively enhancing overall information diversity. Our experimental results further validate the effectiveness of the greedy algorithm.

At the initial stage of the greedy algorithm, we quantify pairwise relationships among visual tokens by constructing a cosine similarity matrix  $C \in \mathbb{R}^{N_1 \times N_1}$ . Each element  $C_{ij}$  of the matrix  $C$  represents the similarity between tokens  $x_i^v$  and  $x_j^v$ . Based on this matrix, we compute the average similarity of each token with all others. The token with the lowest average similarity is chosen as the initial seed to initialize the selected set for the first iteration  $\mathcal{S}^{(1)}$ , and the remaining tokens constitute the initial remaining set  $\mathcal{R}^{(1)}$ . This can be formulated as follows:

$$C_{ij} = \frac{(x_i^v)^\top x_j^v}{\|x_i^v\|_2 \cdot \|x_j^v\|_2} \quad (8)$$

$$c_i^{(1)} = \frac{1}{N_1} \sum_{j=1}^{N_1} C_{ij}, \quad \forall i \in [N_1] \quad (9)$$

$$s^{(1)} = \arg \min_{i \in [N_1]} c_i^{(1)} \quad (10)$$

$$\mathcal{S}^{(1)} = \{s^{(1)}\} \quad \mathcal{R}^{(1)} = [N_1] \setminus \{s^{(1)}\} \quad (11)$$

where  $c_i^{(1)}$  denotes the average similarity between token  $x_i^v$  and the other  $N_1$  visual tokens. The index  $s^{(1)}$  corresponds to the initial token selected as the least similar on average to all others, and  $[N_1]$  denotes the set of indexes from 1 to  $N_1$ . To enable efficient incremental computation, we maintain a similarity accumulation vector  $\sigma \in \mathbb{R}^{N_1}$ , where each element  $\sigma_i$  denotes the average similarity between token  $x_i^v$  and all tokens in the selected set. The initial similarity accumulation vector  $\sigma^{(1)}$  is given by the similarity between the token indexed by  $s^{(1)}$  and all other tokens, which can be represented as follows:

$$\sigma^{(1)} = C_{s^{(1)}}; \quad (12)$$

where  $C_{s^{(1)}};$  denotes the row vector in the matrix  $C$  corresponding to the index  $s^{(1)}$ .

At each iteration  $t = 2, \dots, N_2$ , we compute the average similarity between each remaining token and all tokens in the current selected set. The remaining token with the lowest average similarity is selected in this iteration, and its index is used to update both the selected and remaining sets. Meanwhile, the total similarity accumulation vector is incrementally updated to incorporate the newly selected token. This process is formalized as follows:

$$c_i^{(t)} = \frac{1}{t-1} \cdot \sigma_i^{(t-1)}, \quad \forall i \in \mathcal{R}^{(t-1)} \quad (13)$$

$$s^{(t)} = \arg \min_{i \in \mathcal{R}^{(t-1)}} c_i^{(t)} \quad (14)$$

$$\mathcal{S}^{(t)} = \mathcal{S}^{(t-1)} \cup \{s^{(t)}\}, \quad \mathcal{R}^{(t)} = \mathcal{R}^{(t-1)} \setminus \{s^{(t)}\} \quad (15)$$

$$\sigma^{(t)} = \sigma^{(t-1)} + C_{s^{(t)}}; \quad (16)$$

Here,  $\mathcal{S}^{(t)}$  and  $\mathcal{R}^{(t)}$  denote the selected and remaining sets after the  $t$ -th iteration, respectively.  $c_i^{(t)}$  represents the average similarity between the token  $x_i^v$  in the remaining set and all tokens in the selected set at iteration  $t$ . The index  $s^{(t)}$  corresponds to the token selected during the  $t$ -th iteration, and  $C_{s^{(t)}}$  denotes the row vector in the matrix  $C$  corresponding to the index  $s^{(t)}$ . The similarity accumulation vector  $\sigma^{(t)}$  is updated using the similarity vector  $C_{s^{(t)}}$  of the newly selected token.

This process is repeated  $N_2$  times until  $N_2$  tokens have been selected. The resulting set  $\mathcal{X}^{v(2)} \subset \mathcal{X}^{v(1)}$  forms a maximally dispersed subset of visual tokens with minimal internal redundancy.

## Experiments

### Experimental Setup

**Models and Baselines.** We evaluate the performance of our method across several representative LMMs, including LLaVA-1.5-7B (Liu et al. 2023), LLaVA-1.5-13B (Liu et al. 2023), LLaVA-NEXT-7B (Liu et al. 2024b), LLaVA-NEXT-Video-7B (Zhang et al. 2024c) and Qwen2-VL-7B (Wang et al. 2024). These models span a range of parameter scales and encompass both image and video understanding tasks. We evaluate our method alongside several widely adopted baselines, including ToMe (Bolya et al. 2023), FastV (Chen et al. 2024a), SparseVLM (SpVLM) (Zhang et al. 2024b), PDrop (Xing et al. 2024) and DivPrune (Alvar et al. 2025). We additionally include the VTW (Lin et al. 2025b) method in our efficiency evaluation. All baselines are assessed under consistent experimental settings.

**Datasets and Metrics.** We evaluate our method on diverse multimodal benchmarks covering various tasks. For ChartQA (Masry et al. 2022), we report the relaxed score. Image captioning quality and diversity are measured by CIDEr on COCO (Sharma et al. 2018) and NoCaps (Agrawal et al. 2019). MMBenchEN (MMB) (Liu et al. 2024d) uses a GPT-based score. Perceptual understanding is assessed via the perception score on MME (Fu et al. 2023). Accuracy evaluates general reasoning on MMU (Zheng et al. 2025) and text recognition on OCRBench (Liu et al. 2024e). Exact match accuracy measures question answering on VQAoK (Marino et al. 2019) and VQAtext (Singh et al. 2019). POPE (Li et al. 2023b) is evaluated with precision for positional understanding. This comprehensive protocol ensures thorough assessment of generalization across multimodal tasks.

**Implementation Details.** Our experiments are conducted using the PyTorch framework (Paszke et al. 2019) and the Hugging Face Transformers library (Wolf et al. 2020). We utilize an NVIDIA H100 GPU with 80GB of memory. Moreover, we use scikit-learn (Pedregosa et al. 2011) to compute mutual information, where the library employs a nonparametric  $k$  nearest neighbors approximation method, with  $k$  set to 3 by default. We set the parameter  $N_1 = \lfloor 0.8N \rfloor$  by

default. In both the ablation study and case study, we fix the final number of retained tokens to 64.

### Image Language Understanding

We conduct a comprehensive evaluation of our visual token pruning approach against several baselines. As shown in Table 1, our method consistently outperforms prior works across a range of token retention ratios on LLaVA-1.5-7B. At a moderate retention of 192 tokens, our approach achieves an MME perception score of 1467.30, with only a 2.7% drop relative to the dense model, compared to 13.7% and 16.2% drops for FastV and ToMe, respectively. Compared with the strongest baseline, DivPrune, our method improves MMB accuracy from 62.28 to 63.75, a relative gain of 2.4%. Moreover, the standard deviation of our results is smaller than that of other methods; for example, on ChartQA, our method achieves a standard deviation of 0.75, compared to 0.78 for DivPrune. To further assess the scalability of our approach on larger models, we extend our evaluation to LLaVA-1.5-13B and conduct a comparative analysis against DivPrune under varying visual token retention settings. As presented in Table 2, our method consistently surpasses DivPrune, demonstrating its effectiveness at higher model scale. In particular, on the MMB benchmark, our method achieves a notable score of 67.35 with only 144 retained tokens, outperforming DivPrune’s 66.41 under the same setting. These results highlight the generalization ability of our pruning strategy in large scale settings.

In addition, we conduct experiments on LLaVA-NEXT-7B using a larger pool of visual tokens across different retention settings. As shown in Table 3, our method consistently achieves the strongest performance across a range of compression levels. Furthermore, our experiments on Qwen2-VL-7B also demonstrate the effectiveness of the proposed method (see Appendix 5).

### Video Language Understanding

In this section, we evaluate our method on the video based multimodal model LLaVA-NEXT-Video-7B. Using the same pruning strategy as in our image understanding experiments, we conduct evaluations on the COCO dataset and report standard image captioning metrics, including BLEU-1/2/3/4, ROUGE-L and CIDEr. We compare our method against DivPrune, a strong baseline for visual token pruning. As shown in Table 4, our approach consistently outperforms DivPrune across all evaluation metrics under various token retention settings. For instance, with 960 tokens retained, our method improves the BLEU-4 score from 28.46 to 30.41, representing a relative gain of 6.9%. These results demonstrate the robustness of our method in video scenarios.

### Efficiency Analysis (Accounting for Pruning Overhead)

In this section, we evaluate the inference efficiency of our method on LLaVA-NEXT-7B using the MME dataset. We repeat the process three times and report the average result. As shown in Table 5, we report the average inference time (time to generate the complete output) per sample with a

Method	ChartQA	COCO	MMB	MME	MMU	NoCaps	OCRB	VQAOK	POPE	VQATEXT
<i>Upper Bound, 576 Tokens (100%)</i>										
Dense	18.20	1.10	64.09	1508.24	36.33	1.06	31.30	53.44	93.86	46.11
<i>Retain 192 Tokens (↓ 66.7%)</i>										
ToMe	15.45	0.08	58.64	1262.74	31.49	0.08	29.19	46.88	77.64	39.60
FastV	15.24	0.08	63.06	1302.33	31.26	0.09	29.53	47.24	69.49	38.43
SpVLM	17.17	1.05	61.62	1390.39	35.55	1.00	30.16	50.47	89.66	42.00
PDrop	17.06	1.06	60.41	1426.75	34.42	0.99	30.35	50.83	88.26	41.78
DivPrune	17.40	1.06	62.29	1436.44	35.78	1.01	30.40	51.55	91.37	43.24
<b>Ours</b>	<b>17.80</b>	<b>1.08</b>	<b>63.75</b>	<b>1467.30</b>	<b>36.22</b>	<b>1.03</b>	<b>31.00</b>	<b>52.29</b>	<b>93.68</b>	<b>45.10</b>
<i>Retain 128 Tokens (↓ 77.8%)</i>										
ToMe	14.13	0.06	57.27	1066.04	30.69	0.06	24.93	43.24	68.92	37.90
FastV	13.86	0.07	<b>62.89</b>	1182.73	31.71	0.08	26.24	44.56	65.41	35.88
SpVLM	16.56	1.04	60.08	1346.25	33.85	1.01	28.06	48.35	88.35	40.51
PDrop	16.35	1.03	59.97	1320.85	34.76	1.01	28.81	49.85	90.32	41.30
DivPrune	16.96	1.04	61.77	1396.25	36.22	<b>1.04</b>	29.00	50.02	91.31	41.66
<b>Ours</b>	<b>17.80</b>	<b>1.06</b>	62.80	<b>1397.22</b>	<b>36.44</b>	1.02	<b>29.50</b>	<b>51.12</b>	<b>94.29</b>	<b>44.28</b>
<i>Retain 64 Tokens (↓ 88.9%)</i>										
ToMe	12.49	0.05	49.97	909.99	27.46	0.06	20.07	39.47	62.85	34.59
FastV	12.03	0.05	58.94	1004.35	29.40	0.06	22.04	41.65	57.46	32.81
SpVLM	14.92	0.99	58.03	1203.46	26.55	0.95	25.81	45.14	89.91	37.51
PDrop	15.14	0.99	45.42	1248.24	34.98	0.94	27.00	44.09	66.92	33.81
DivPrune	15.84	0.99	59.28	1348.99	35.89	0.94	27.60	48.36	92.18	39.22
<b>Ours</b>	<b>16.36</b>	<b>1.02</b>	<b>61.34</b>	<b>1359.12</b>	<b>36.11</b>	<b>0.98</b>	<b>29.00</b>	<b>49.37</b>	<b>95.01</b>	<b>41.45</b>

Table 1: Comparison of visual token pruning methods on LLaVA-1.5-7B across multiple benchmarks under varying token retention ratios. Best results are highlighted in bold.

Method	ChartQA	COCO	MMB	NoCaps	OCRB	POPE
<i>Upper Bound, 576 Tokens (100%)</i>						
Dense	18.20	1.16	68.73	1.09	33.60	94.44
<i>Retain 144 Tokens (↓ 75.0%)</i>						
DivPrune	17.28	1.09	66.41	1.02	31.10	94.63
<b>Ours</b>	<b>17.44</b>	<b>1.10</b>	<b>67.35</b>	<b>1.04</b>	<b>33.00</b>	<b>96.69</b>
<i>Retain 128 Tokens (↓ 77.8%)</i>						
DivPrune	17.08	1.09	66.07	1.01	30.90	94.76
<b>Ours</b>	<b>17.88</b>	<b>1.09</b>	<b>66.84</b>	<b>1.04</b>	<b>33.10</b>	<b>96.55</b>
<i>Retain 64 Tokens (↓ 88.9%)</i>						
DivPrune	16.32	1.03	64.52	0.97	30.10	95.84
<b>Ours</b>	<b>16.56</b>	<b>1.05</b>	<b>64.95</b>	<b>0.99</b>	<b>30.60</b>	<b>97.63</b>

Table 2: Comparison between our visual token pruning method and DivPrune on LLaVA-1.5-13B across multiple benchmarks under varying token retention settings.

batch size of 1 and 288 visual tokens retained. Compared to the original dense model (15.53 GB, 235.2 ms), all pruning methods significantly reduce memory usage and cut inference latency by more than half. Our method achieves an inference time of 100.13 ms, representing a 57% reduction compared to the dense baseline. When compared with other pruning baselines, our approach achieves lower latency than VTV and FastV. Although our latency is slightly higher than DivPrune, this small gap is negligible given the supe-

rior task performance consistently achieved under the same token budget. It is worth noting that pruning is performed during inference; therefore, the reported inference latency includes the overhead introduced by the pruning process. These results demonstrate that our pruning strategy provides substantial improvements in memory and latency efficiency.

### Ablation Study

**Cross-Modal Token Filtering.** To assess the effectiveness of the proposed cross-modal alignment aware token filtering strategy, we perform an ablation study on LLaVA-1.5-7B across several representative benchmarks. As shown in Figure 2, we evaluate three configurations: the original dense model, a pruning variant without cross-modal filtering, and our pruning approach incorporating cross-modal filtering. The experimental results clearly demonstrate that our method successfully eliminates redundant visual tokens while minimizing performance degradation. Compared to the dense baseline, our approach consistently maintains competitive performance across all benchmarks, exhibiting only marginal declines. In contrast, the pruning strategy without cross-modal filtering suffers from noticeably larger performance drops, underscoring the critical role of cross-modal alignment in preserving model performance during token compression.

Additionally, we conduct ablation studies to validate the effectiveness of our intra-modal representation maximization strategy and the  $L_2$  norm based mutual information approximation (Appendix 2).

Method	ChartQA	COCO	MME	NoCaps	OCRB	POPE
<i>Upper Bound, 2880 Tokens (100%)</i>						
Dense	54.88	1.00	1519.30	0.88	52.50	95.71
<i>Retain 720 Tokens (↓ 75.0%)</i>						
ToMe	36.57	0.08	1294.12	0.09	42.25	81.58
FastV	36.09	0.09	1334.69	0.10	42.74	73.01
SpVLM	40.66	0.95	1424.94	0.82	43.65	94.20
PDrop	40.39	0.95	1462.20	0.83	43.93	92.73
DivPrune	41.20	0.95	1472.13	0.83	44.00	96.00
<b>Ours</b>	<b>44.92</b>	<b>1.00</b>	<b>1503.24</b>	<b>0.86</b>	<b>46.40</b>	<b>96.44</b>
<i>Retain 640 Tokens (↓ 77.8%)</i>						
ToMe	32.43	0.08	1133.13	0.08	37.05	72.73
FastV	31.82	0.08	1257.15	0.09	39.00	69.02
SpVLM	37.99	0.94	1430.96	0.83	41.71	93.22
PDrop	37.53	0.94	1403.96	0.82	42.82	95.31
DivPrune	38.92	0.96	1484.12	0.83	43.10	96.35
<b>Ours</b>	<b>43.72</b>	<b>0.99</b>	<b>1492.60</b>	<b>0.99</b>	<b>45.10</b>	<b>96.76</b>
<i>Retain 320 Tokens (↓ 88.9%)</i>						
ToMe	25.27	0.08	976.13	0.08	25.23	66.17
FastV	24.34	0.08	1077.35	0.08	27.71	60.50
SpVLM	30.18	0.92	1290.93	0.80	32.45	94.66
PDrop	30.62	0.92	1338.97	0.80	33.95	70.46
DivPrune	32.04	0.93	1447.05	0.80	34.70	<b>97.05</b>
<b>Ours</b>	<b>35.64</b>	<b>0.96</b>	<b>1452.37</b>	<b>0.82</b>	<b>37.90</b>	96.47

Table 3: Performance comparison of our visual token pruning method with other baselines on LLaVA-NEXT-7B across multiple benchmarks under varying token retention settings (retaining 720, 640, and 320 tokens).

Method	B-1	B-2	B-3	B-4	R-L	CIDEr
<i>Upper Bound, 2880 Tokens (100%)</i>						
Dense	71.07	54.78	40.50	29.24	53.58	1.02
<i>Retain 960 Tokens (↓ 66.7%)</i>						
DivPrune	72.51	54.97	40.00	28.46	53.79	0.99
<b>Ours</b>	<b>73.27</b>	<b>56.63</b>	<b>42.03</b>	<b>30.41</b>	<b>54.67</b>	<b>1.04</b>
<i>Retain 720 Tokens (↓ 75.0%)</i>						
DivPrune	72.35	54.81	39.88	28.37	53.61	0.99
<b>Ours</b>	<b>72.87</b>	<b>56.34</b>	<b>41.77</b>	<b>30.23</b>	<b>54.47</b>	<b>1.04</b>
<i>Retain 540 Tokens (↓ 81.3%)</i>						
DivPrune	71.72	54.16	39.21	27.75	53.28	0.98
<b>Ours</b>	<b>72.34</b>	<b>55.55</b>	<b>40.92</b>	<b>29.47</b>	<b>53.75</b>	<b>1.03</b>
<i>Retain 480 Tokens (↓ 83.3%)</i>						
DivPrune	71.28	53.72	38.88	27.47	53.13	0.97
<b>Ours</b>	<b>72.44</b>	<b>55.49</b>	<b>40.74</b>	<b>29.21</b>	<b>53.80</b>	<b>1.01</b>

Table 4: Performance comparison of our visual token pruning method and DivPrune on LLaVA-NEXT-Video-7B, evaluated on COCO using standard captioning metrics. B denotes BLEU, and R denotes ROUGE.

Method	Memory (G)	Latency (ms)
Dense	15.53	235.2
VTW	13.63	103.71
FastV	13.63	108.29
DivPrune	13.63	99.53
<b>Ours</b>	13.63	100.13

Table 5: Comparison of peak GPU memory usage and average per-sample latency for our pruning method and baselines on LLaVA-NEXT-7B, evaluated on the MME dataset with a batch size of 1 and 288 retained visual tokens.

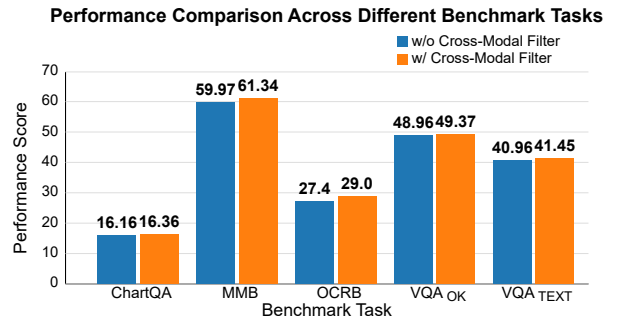


Figure 2: Ablation study on the impact of cross-modal alignment aware token filtering in LLaVA-1.5-7B across multiple benchmarks.

## Additional Results

We conduct a **Hyperparameter Analysis**, such as varying  $N_1$ , and observe consistently strong performance across different settings, demonstrating the robustness of our method (Appendix 3). Moreover, we perform a **Case Study** to show that the pruned model retains its ability to generate high quality content (Appendix 4).

## Conclusion

In this paper, we analyze the redundancy discrepancy between visual and textual tokens in LMMs and propose a pruning strategy that operates exclusively on visual tokens. Our method explicitly preserves cross-modal alignment and intra-modal informational diversity. Specifically, we leverage mutual information to eliminate visual tokens that are semantically misaligned with textual inputs, ensuring the consistency across modalities. To further enhance the representational quality of the retained tokens, we maximize their expected pairwise distances in the embedding space via an efficient greedy algorithm. Extensive experiments across diverse models and benchmarks demonstrate the effectiveness of our approach, alongside significant improvements in memory consumption and inference latency. We plan to extend our approach to more complex or non-visual modalities in future work, further demonstrating its broad applicability.

## References

Adamic, L. A.; and Huberman, B. A. 2002. Zipf's law and the Internet. *Glottometrics*, 3(1): 143–150.

Agrawal, H.; Desai, K.; Wang, Y.; Chen, X.; Jain, R.; Johnson, M.; Batra, D.; Parikh, D.; Lee, S.; and Anderson, P. 2019. Nocaps: Novel object captioning at scale. In *Proceedings of the IEEE/CVF international conference on computer vision*, 8948–8957.

Alvar, S. R.; Singh, G.; Akbari, M.; and Zhang, Y. 2025. DivPrune: Diversity-based Visual Token Pruning for Large Multimodal Models. *arXiv preprint arXiv:2503.02175*.

Bai, S.; Chen, K.; Liu, X.; Wang, J.; Ge, W.; Song, S.; Dang, K.; Wang, P.; Wang, S.; Tang, J.; et al. 2025. Qwen2. 5-vl technical report. *arXiv preprint arXiv:2502.13923*.

Bolya, D.; Fu, C.-Y.; Dai, X.; Zhang, P.; Feichtenhofer, C.; and Hoffman, J. 2023. Token merging: Your vit but faster. In *Proceedings of the International Conference on Learning Representations*.

Brown, T.; Mann, B.; Ryder, N.; Subbiah, M.; Kaplan, J.; Dhariwal, P.; Neelakantan, A.; Shyam, P.; Sastry, G.; Askell, A.; et al. 2020. Language models are few-shot learners. *Advances in neural information processing systems* 33.

Cai, M.; Yang, J.; Gao, J.; and Lee, Y. J. 2024. Matryoshka multimodal models. In *Workshop on Video-Language Models@NeurIPS 2024*.

Chebotar, Y.; Vuong, Q.; Hausman, K.; Xia, F.; Lu, Y.; Irpan, A.; Kumar, A.; Yu, T.; Herzog, A.; Pertsch, K.; et al. 2023. Q-transformer: Scalable offline reinforcement learning via autoregressive q-functions. In *Conference on Robot Learning*, 3909–3928. PMLR.

Chen, K.; Li, J.; Li, Y.; and Li, Z. 2023. A Survey on Efficient Transformer Models.

Chen, L.; Zhao, H.; Liu, T.; Bai, S.; Lin, J.; Zhou, C.; and Chang, B. 2024a. An image is worth 1/2 tokens after layer 2: Plug-and-play inference acceleration for large vision-language models. In *European Conference on Computer Vision*, 19–35. Springer.

Chen, L.; Zhao, H.; Liu, T.; Bai, S.; Lin, J.; Zhou, C.; and Chang, B. 2024b. An image is worth 1/2 tokens after layer 2: Plug-and-play inference acceleration for large vision-language models. In *European Conference on Computer Vision*, 19–35. Springer.

Chiang, W.-L.; Li, Z.; Lin, Z.; Sheng, Y.; Wu, Z.; Zhang, H.; Zheng, L.; Zhuang, S.; Zhuang, Y.; Gonzalez, J. E.; et al. 2023. Vicuna: An open-source chatbot impressing gpt-4 with 90%\* chatgpt quality. *See https://vicuna.lmsys.org (accessed 14 April 2023)*, 2(3): 6.

Covert, I.; Sun, T.; Zou, J.; and Hashimoto, T. 2024. Locality Alignment Improves Vision-Language Models. *arXiv preprint arXiv:2410.11087*.

Face, H. 2024. *Mastering Transformers: The Journey from BERT to Large Language Models and Stable Diffusion*. Open Library.

Fu, C.; Chen, P.; Shen, Y.; Qin, Y.; Zhang, M.; Lin, X.; Qiu, Z.; Lin, W.; Yang, J.; Zheng, X.; Li, K.; Sun, X.; and Ji, R. 2023. MME: A Comprehensive Evaluation Benchmark for Multimodal Large Language Models. *ArXiv*, abs/2306.13394.

Hirschberg, J.; and Manning, C. D. 2015. Advances in natural language processing. *Science*, 349(6245): 261–266.

Huang, E.; et al. 2023. Evaluating Large Language Models in Complex Scenarios. *Journal of Computational Linguistics*.

Huang, K.; Zou, H.; Xi, Y.; Wang, B.; Xie, Z.; and Yu, L. 2024. Ivtp: Instruction-guided visual token pruning for large vision-language models. In *European Conference on Computer Vision*, 214–230. Springer.

Keles, F. D.; Wijewardena, P. M.; and Hegde, C. 2023. On the computational complexity of self-attention. In *International conference on algorithmic learning theory*, 597–619. PMLR.

Koonce, B. 2021. ResNet 50. In *Convolutional neural networks with swift for tensorflow: image recognition and dataset categorization*, 63–72. Springer.

Lee, J.; Xuan, K.; Ekbote, C.; Polisetty, S.; Fung, Y. R.; and Liang, P. P. 2025. TAMP: Token-Adaptive Layerwise Pruning in Multimodal Large Language Models. *arXiv preprint arXiv:2504.09897*.

Li, C.; et al. 2023a. Fine-Tuning Techniques for Efficient Model Adaptation. *AI Research Journal*.

Li, D.; Yang, Z.; and Lu, S. 2025. ToDRE: Visual Token Pruning via Diversity and Task Awareness for Efficient Large Vision-Language Models. *arXiv preprint arXiv:2505.18757*.

Li, M.; Su, N.; Qu, F.; Zhong, Z.; Chen, Z.; Li, Y.; Tu, Z.; and Li, X. 2025a. VISTA: Enhancing Vision-Text Alignment in MLLMs via Cross-Modal Mutual Information Maximization. *arXiv preprint arXiv:2505.10917*.

Li, W.; Yuan, Y.; Liu, J.; Tang, D.; Wang, S.; Qin, J.; Zhu, J.; and Zhang, L. 2025b. Tokenpacker: Efficient visual projector for multimodal llm. *International Journal of Computer Vision*, 1–19.

Li, Y.; Du, Y.; Zhou, K.; Wang, J.; Zhao, W. X.; and Wen, J.-R. 2023b. Evaluating object hallucination in large vision-language models. *arXiv preprint arXiv:2305.10355*.

Lin, B.; Ye, Y.; Zhu, B.; Cui, J.; Ning, M.; Jin, P.; and Yuan, L. 2023. Video-llava: Learning united visual representation by alignment before projection. *arXiv preprint arXiv:2311.10122*.

Lin, Z.; Lin, M.; Lin, L.; and Ji, R. 2025a. Boosting multimodal large language models with visual tokens withdrawal for rapid inference. In *Proceedings of the AAAI Conference on Artificial Intelligence*, 5334–5342.

Lin, Z.; Lin, M.; Lin, L.; and Ji, R. 2025b. Boosting multimodal large language models with visual tokens withdrawal for rapid inference. In *Proceedings of the AAAI Conference on Artificial Intelligence*, volume 39, 5334–5342.

Liu, H.; Li, C.; Li, Y.; and Lee, Y. J. 2024a. Improved baselines with visual instruction tuning. In *Proceedings of the IEEE/CVF Conference on Computer Vision and Pattern Recognition*, 26296–26306.

Liu, H.; Li, C.; Li, Y.; Li, B.; Zhang, Y.; Shen, S.; and Lee, Y. J. 2024b. Llavanext: Improved reasoning, ocr, and world knowledge.

Liu, H.; Li, C.; Wu, Q.; and Lee, Y. J. 2023. Visual instruction tuning. *Advances in neural information processing systems*, 36: 34892–34916.

Liu, S.; Yu, H.; Liao, C.; Li, J.; Lin, W.; Liu, A. X.; and Dustdar, S. 2022. Pyraformer: Low-complexity pyramidal attention for long-range time series modeling and forecasting. In *# PLACEHOLDER\_PARENT\_METADATA\_VALUE#*.

Liu, T.; Shi, L.; Hong, R.; Hu, Y.; Yin, Q.; and Zhang, L. 2024c. Multi-Stage Vision Token Dropping: Towards Efficient Multimodal Large Language Model. *arXiv preprint arXiv:2411.10803*.

Liu, Y.; Duan, H.; Zhang, Y.; Li, B.; Zhang, S.; Zhao, W.; Yuan, Y.; Wang, J.; He, C.; Liu, Z.; et al. 2024d. Mmbench: Is your multi-modal model an all-around player? In *European conference on computer vision*, 216–233. Springer.

Liu, Y.; Li, Z.; Huang, M.; Yang, B.; Yu, W.; Li, C.; Yin, X.-C.; Liu, C.-L.; Jin, L.; and Bai, X. 2024e. Ocrbench: on the hidden mystery of ocr in large multimodal models. *Science China Information Sciences*, 67(12): 220102.

Marino, K.; Rastegari, M.; Farhadi, A.; and Mottaghi, R. 2019. Ok-vqa: A visual question answering benchmark requiring external knowledge. In *Proceedings of the IEEE/cvf conference on computer vision and pattern recognition*, 3195–3204.

Masry, A.; Long, D. X.; Tan, J. Q.; Joty, S.; and Hoque, E. 2022. Chartqa: A benchmark for question answering about charts with visual and logical reasoning. *arXiv preprint arXiv:2203.10244*.

Newman, M. E. 2005. Power laws, Pareto distributions and Zipf's law. *Contemporary physics*, 46(5): 323–351.

Paszke, A.; Gross, S.; Massa, F.; Lerer, A.; Bradbury, J.; Chanan, G.; Killeen, T.; Lin, Z.; Gimelshein, N.; Antiga, L.; et al. 2019. Pytorch: An imperative style, high-performance deep learning library. *Advances in neural information processing systems*, 32.

Pedregosa, F.; Varoquaux, G.; Gramfort, A.; Michel, V.; Thirion, B.; Grisel, O.; Blondel, M.; Prettenhofer, P.; Weiss, R.; Dubourg, V.; et al. 2011. Scikit-learn: Machine learning in Python. *the Journal of machine Learning research*, 12: 2825–2830.

Rusak, E.; Reizinger, P.; Juhos, A.; Bringmann, O.; Zimmermann, R. S.; and Brendel, W. 2024. InfoNCE: Identifying the gap between theory and practice. *arXiv preprint arXiv:2407.00143*.

Shang, Y.; Cai, M.; Xu, B.; Lee, Y. J.; and Yan, Y. 2024a. Llava-prumerge: Adaptive token reduction for efficient large multimodal models. *arXiv preprint arXiv:2403.15388*.

Shang, Y.; Cai, M.; Xu, B.; Lee, Y. J.; and Yan, Y. 2024b. Llava-prumerge: Adaptive token reduction for efficient large multimodal models. *arXiv preprint arXiv:2403.15388*.

Sharma, P.; Ding, N.; Goodman, S.; and Soricut, R. 2018. Conceptual captions: A cleaned, hypernymed, image alt-text dataset for automatic image captioning. In *Proceedings of the 56th Annual Meeting of the Association for Computational Linguistics (Volume 1: Long Papers)*, 2556–2565.

Singh, A.; Natarajan, V.; Shah, M.; Jiang, Y.; Chen, X.; Batra, D.; Parikh, D.; and Rohrbach, M. 2019. Towards vqa models that can read. In *Proceedings of the IEEE/CVF conference on computer vision and pattern recognition*, 8317–8326.

Sun, Y.; Xin, Y.; Li, H.; Lin, C.; and Batista-Navarro, R. ????. VeLAR: Vision-oriEnted Language-Attentive token Reduction for multimodal large language models.

Sun, Y.; Xin, Y.; Li, H.; Sun, J.; Lin, C.; and Batista-Navarro, R. 2025. Lvpruning: An effective yet simple language-guided vision token pruning approach for multi-modal large language models. *arXiv preprint arXiv:2501.13652*.

Taud, H.; and Mas, J.-F. 2017. Multilayer perceptron (MLP). In *Geomatic approaches for modeling land change scenarios*, 451–455. Springer.

Team, K.; Du, A.; Yin, B.; Xing, B.; Qu, B.; Wang, B.; Chen, C.; Zhang, C.; Du, C.; Wei, C.; et al. 2025. Kimi-vl technical report. *arXiv preprint arXiv:2504.07491*.

Tong, J.; Jin, W.; Qin, P.; Li, A.; Zou, Y.; Li, Y.; Li, Y.; and Li, R. 2025. FlowCut: Rethinking Redundancy via Information Flow for Efficient Vision-Language Models. *arXiv preprint arXiv:2505.19536*.

Touvron, H.; Lavril, T.; Izacard, G.; Martinet, X.; Lachaux, M.; Lacroix, T.; Rozière, B.; Goyal, N.; Hambro, E.; Azhar, F.; et al. 2023. Open and efficient foundation language models. *Preprint at arXiv. https://doi. org/10.48550/arXiv*, 2302.

Vaswani, A.; Shazeer, N.; Parmar, N.; Uszkoreit, J.; Jones, L.; Gomez, A. N.; Kaiser, L.; and Polosukhin, I. 2017. Attention Is All You Need.

Wang, F.; et al. 2023. Practical Applications of LLMs in Specialized Domains. *Specialized AI Applications*.

Wang, P.; Bai, S.; Tan, S.; Wang, S.; Fan, Z.; Bai, J.; Chen, K.; Liu, X.; Wang, J.; Ge, W.; et al. 2024. Qwen2-vl: Enhancing vision-language model's perception of the world at any resolution. *arXiv preprint arXiv:2409.12191*.

Wolf, T.; Debut, L.; Sanh, V.; Chaumond, J.; Delangue, C.; Moi, A.; Cistac, P.; Rault, T.; Louf, R.; Funtowicz, M.; et al. 2020. Transformers: State-of-the-art natural language processing. In *Proceedings of the 2020 conference on empirical methods in natural language processing: system demonstrations*, 38–45.

Xing, L.; Huang, Q.; Dong, X.; Lu, J.; Zhang, P.; Zang, Y.; Cao, Y.; He, C.; Wang, J.; Wu, F.; et al. 2024. Pyramiddrop: Accelerating your large vision-language models via pyramid visual redundancy reduction. *arXiv preprint arXiv:2410.17247*.

Yang, S.; Chen, Y.; Tian, Z.; Wang, C.; Li, J.; Yu, B.; and Jia, J. 2025. Visionzip: Longer is better but not necessary in vision language models. In *Proceedings of the Computer Vision and Pattern Recognition Conference*, 19792–19802.

Ye, W.; Wu, Q.; Lin, W.; and Zhou, Y. 2025. Fit and prune: Fast and training-free visual token pruning for multi-modal large language models. In *Proceedings of the AAAI Conference on Artificial Intelligence*, 22128–22136.

Yin, H.; Vahdat, A.; Alvarez, J. M.; Mallya, A.; Kautz, J.; and Molchanov, P. 2022. A-vit: Adaptive tokens for efficient

vision transformer. In *Proceedings of the IEEE/CVF conference on computer vision and pattern recognition*, 10809–10818.

Yuan, L.; Chen, Y.; Wang, T.; Yu, W.; Shi, Y.; Jiang, Z.-H.; Tay, F. E.; Feng, J.; and Yan, S. 2021. Tokens-to-token vit: Training vision transformers from scratch on imagenet. In *Proceedings of the IEEE/CVF international conference on computer vision*, 558–567.

Zhang, D.; et al. 2023. Parameter-Efficient Fine-Tuning Methods for LLMs. *Journal of Machine Learning Research*.

Zhang, Q.; Cheng, A.; Lu, M.; Zhuo, Z.; Wang, M.; Cao, J.; Guo, S.; She, Q.; and Zhang, S. 2024a. [CLS] Attention is All You Need for Training-Free Visual Token Pruning: Make VLM Inference Faster. *arXiv preprint arXiv:2412.01818*.

Zhang, Q.; Liu, M.; Li, L.; Lu, M.; Zhang, Y.; Pan, J.; She, Q.; and Zhang, S. 2025. Beyond Attention or Similarity: Maximizing Conditional Diversity for Token Pruning in MLLMs. *arXiv preprint arXiv:2506.10967*.

Zhang, Y.; Fan, C.-K.; Ma, J.; Zheng, W.; Huang, T.; Cheng, K.; Gudovskiy, D.; Okuno, T.; Nakata, Y.; Keutzer, K.; et al. 2024b. Sparsevlm: Visual token sparsification for efficient vision-language model inference. *arXiv preprint arXiv:2410.04417*.

Zhang, Y.; Li, B.; Liu, h.; Lee, Y. j.; Gui, L.; Fu, D.; Feng, J.; Liu, Z.; and Li, C. 2024c. LLaVA-NeXT: A Strong Zero-shot Video Understanding Model.

Zheng, L.; Fei, H.; Dai, T.; Peng, Z.; Li, F.; Ma, H.; Teng, C.; and Ji, D. 2025. Multi-Granular Multimodal Clue Fusion for Meme Understanding. In *Proceedings of the AAAI Conference on Artificial Intelligence*, volume 39, 26057–26065.

Zhu, B.; et al. 2023. Expanding Frontiers in Large Language Models. *AI Frontier Research*.

Zhu, J.; Wang, W.; Chen, Z.; Liu, Z.; Ye, S.; Gu, L.; Duan, Y.; Tian, H.; Su, W.; Shao, J.; et al. 2025. InternVL3: Exploring Advanced Training and Test-Time Recipes for Open-Source Multimodal Models. *arXiv preprint arXiv:2504.10479*.